Automated heterodyne method to characterize semiconductor based akinetic swept laser sources

Carlos Reyes[a], Tomasz Piwonski[a,b], Brian Corbett[a], and Brendan Roycroft[a]

[a]Tyndall National Institute, University College Cork, Lee Maltings, Cork, Ireland
[b]CAPPA - Centre for Advanced Photonics & Process Analysis, Cork Institute of Technology, Bishopstown, Cork, Ireland

ABSTRACT

An automated heterodyne method is proposed to characterize sampled grating distributed Bragg reflector (SG-DBR) lasers in terms of their lasing output wavelength, side-mode suppression ratio (SMSR) and output power. Such lasers are the core of akinetic all-semiconductor based swept sources for Optical Coherence Tomography (OCT) systems. The purpose of the paper is to demonstrate the technique and obtain a broader optical and electrical understanding in DC and AC operation. A JDSU Agile SG-DBR laser was characterized and found to have a tuning range $\approx$ 60 nm, a center wavelength $\lambda_c = 1540$ nm and average lasing power of 10 mW. The result of the AC characterization is a 'tuning dictionary' that contains 379 tuning points (10 μs per tuning point).

Keywords: Optical coherence tomography, swept sources, telecoms lasers, tunable lasers

1. INTRODUCTION

Optical Coherence Tomography (OCT) is proven to be a non-invasive, high resolution (1-15 μm) medical optical imaging technology capable of providing cross-sectional images to visualize the structure of biological samples as well as internal body organs.[1] OCT has evolved from Time Domain (TD-OCT)[2] to Fourier Domain OCT (FD-OCT) techniques: Spectral Domain OCT (SD-OCT)[3–5] and Swept Source OCT (SS-OCT).[6–9] Both SD-OCT and SS-OCT obtain depth profiles (A-scans) by Fourier transforming a wavelength dependent reflectivity profile, however the profile is obtained in different ways. SD-OCT uses a broad band light source and a spectrometer with a camera, with the readout time of the camera being its main speed limitation. SS-OCT addresses this limitation by using a swept source that is able to rapidly tune/sweep a narrow band laser light over a large optical bandwidth and a single balanced photodetector on the receive side.[10] Wavelength-tuning speed, tuning range, linewidth and single-mode operation are critical factors in SS-OCT.

Different commercial swept source technologies are available in the market.[11,12] Each source has particular advantages in terms of scanning speed, wavelength coverage, center wavelength and output power. Out of the available sources, akinetic all-semiconductor technology based on wafer-scale laser fabrication can potentially reduce the price of swept sources due to high-volume manufacturing of telecoms suppliers as the core of the swept source is a Sampled Grating Distributed Bragg Reflector (SG-DBR)[13–15] commonly used in telecoms applications such as wavelength division multiplexing (WDM).[16] Despite such advantages, SG-DBR lasers have insufficient functionality for OCT applications, e.g., invalid points in the sweep, poor quality of the point spread function (PSF) and large stitching noise.[17] In order for akinetic swept sources to be established as the future core technology of SS-OCT these limitations have to be well understood. Hence, this paper explains the electronic and optical limitations of SG-DBR lasers such as electronic switching speed, electric noise, mode-hopping and tuning range in order to provide a broader understanding to swept source researchers in terms of its lasing output wavelength, side-mode suppression ratio (SMSR) and output power.

Such limitations of the SG-DBR laser can be understood by a DC and AC characterization. DC characterization provides a broad understanding of the behavior of the laser in terms of its tuning range, center wavelength, average power and SMSR. SS-OCT requires swept sources to be tuned dynamically, hence it is necessary to perform AC/dynamic lasing wavelength characterization. This was achieved with the proposed automated heterodyne method which yields a 'tuning dictionary' containing different current combinations that will control the output lasing wavelength of the laser so that the laser sweeps the wavelength in linearly increasing steps. This automated heterodyne method will be a useful tool for swept source researchers in order to characterize tunable lasers intended to be the core laser of akinetic swept sources.

2. METHODS

SS-OCT requires a swept laser that is able to sweep over a wide wavelength range while maintaining low relative intensity noise (RIN), low side modes and adequate coherence length. Each individual wavelength is interfered with a reference mirror and Fourier transformed. Such sweeps have been achieved by commercially available swept sources provided by Axsun Technologies (MEMS tunable filter),[18] EXALOS (MEMS tunable filters),[19] NTT (External resonator),[20] Santec (Polygon Scanners),[21] Thorlabs (VCSEL),[22] Superlum (Acousto-Optical Tunable Filter),[23] Optores (FDML Laser)[24] and Insight Photonic Solutions (Akinetic Semiconductor Laser).[25] In contrast to the swept sources based in mechanical movements, akinetic all-semiconductor technology based on wafer-scale lasers are flexible, compact and can potentially reduce the price of swept source due to high-volume manufacturing of telecoms suppliers.[11] OCT imaging capabilities with such akinetic all-semiconductor swept sources have been proven[26–28] at different sweep rates from 20-200 kHz with different axial resolutions between 10 μm to 20 μm at 1060, 1310 and 1550 nm.

The core laser of akinetic swept sources is an all-semiconductor SG-DBR monolithic tunable laser diode with a tuning range from 1525 to 1565 nm (C-band) or from 1565 to 1605 nm (L-band) at a fast wavelength tuning speed ($\approx$ 5 ns). Lasing is obtained by applying an electric current through the sections of a semiconductor structure: back mirror (BM), phase, gain, front mirror (FM) and semiconductor optical amplifier (SOA), as shown in Fig 1. The injection of electric carriers to each section produces a change in the refractive index, hence a change of the effective optical path length. Each section has a specific purpose. The gain section provides an amplification region for continued lasing in order to obtain stimulated emission. The FM, BM and phase sections control the output wavelength for ideal continuous frequency ramps required by SS-OCT. The FM and BM are sampled grating distributed Bragg reflectors (SG-DBR) that provide broad semi-continuous wavelength tuning (with mode-hopping), whereas the phase section provides fine tuning over a narrow range of continuous tuning, such effect is obtained by modulating the overall effective cavity length. The SOA allows power leveling of the output light, hence it can be used to modulate the output power as desired and is also used as a switch to shutter the output light.

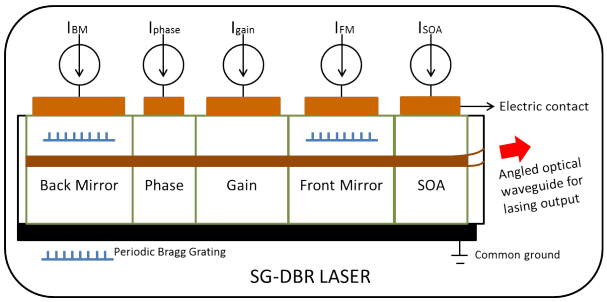

Figure 1. Cross-sectional view of a SG-DBR laser. The laser is composed of five sections: Back Mirror (BM), Phase, Gain, Front Mirror (FM) and Semiconductor Optical Amplifier (SOA). The combination of different values of currents I_{BM}, I_{phase}, I_{gain}, I_{FM} and I_{SOA} determine the lasing wavelength, optical power and side-mode suppression ratio (SMSR).

2.1 Vernier tuning mechanism

Continuous tuning range $\Delta\lambda$ is limited to $\approx$ 15nm as defined by $\Delta\lambda \approx \Delta n/n_g$, where n is the index change and n_g the group index of the tuning sections; such tuning range can be extended by using two or more control variables. These control variables are the front and back mirrors whose structure is a Bragg reflector, an alternating periodic structure of two different optical materials, hence creating a periodic variation of the refractive index and high reflectance at specific wavelength values.[29] Sampled gratings create frequency dependent reflectivity spectra, where the spacing between the peaks is defined by the grating separation. Injection of carriers to both mirrors modifies the mirror spacing through a change in index of refraction, hence producing different wavelength dependent reflectivity profiles. It is this Vernier tuning mechanism on both mirrors that can be used in combination to select the available wavelengths across the tuning band. Due to different periodicity in the reflectivity spectrum only one alignment of the FM and BM peaks will occur.[29] The tuning mechanism is illustrated in Fig. 2.

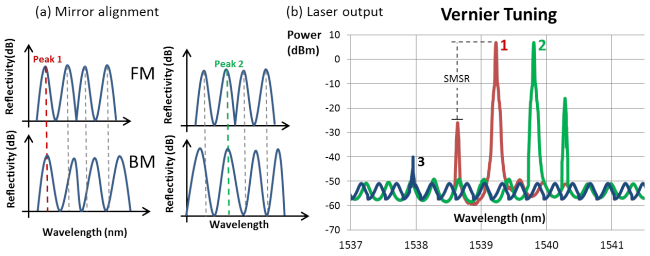

Figure 2. a) Reflectivity spectra defined by the grating spacing. Both spectra can be shifted by injecting carriers in order to obtain different peak alignments. b) The resulting main peaks have a given value of side-mode suppression ratio (SMSR), which is the relation of power between the center peak with the nearest higher order mode.

2.2 Measurement setup

SG-DBR lasers can be characterized in DC and in AC operation. The most basic characterization is to measure the lasing output wavelength, side-mode suppression ratio (SMSR) and output power in DC operation as a function of the FM and BM currents while keeping the rest of the sections biased under a constant current. This output plot is called the tuning map of the laser.[30,31] AC characterization is more complicated as the laser sections have to be dynamically tuned. In order to obtain both measurements a commercial telecoms SG-DBR laser (TLDM-6S Widely Tunable Laser Mode, JDSU Agile) was used in the proposed electro/optical setup (Fig. 3) which is composed of two main blocks: DC characterization and AC characterization.

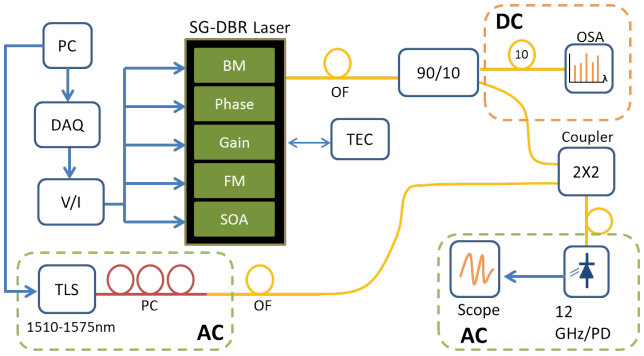

Figure 3. Heterodyne experimental setup. DAQ (Digital-to-Analog); V/I (Voltage-to Current converter); SOA (Semiconductor Optical Amplifier); OSA (Optical Spectrum Analyzer); TLS (Tunable Laser Source); PC (Polarization Controller); OF (Optical Fibre); PD (Photodetector); TEC (Thermo-electric controller).

For the DC characterization setup, a computer controls a Digital-to-Analog converter (DAQ National Instruments, PCI-6733) which generates a signal between 9 and 6 volts. The voltage signal is converted to a current signal through a Voltage-to-Current (V/I) converter, which is then injected to the laser. The SG-DBR laser is fiberized and 10% of its power is connected directly to an Optical Spectrum Analyzer (OSA). The temperature is regulated with a thermo-electric controller (TEC). The results are mapped to two different tuning maps where the output wavelength and SMSR ratio are graphically represented as a function of the current combinations of the mirrors respectively. Such a map can be represented as a matrix (Fig. 4) where the size is determined by the number of steps in both BM and FM, $N_{steps_{BM}}$ and $N_{steps_{FM}}$. The number of steps is defined as $(I_{max} - I_{min})/I_{step}$. DC characterization provides an insight of the laser's behavior, however SS-OCT applications require fast sweeping rates (orders of kHz). Dynamic laser tuning modifies its optical behavior due to limited electronic bandwidth, hysteresis and increase in temperature. For such reason four elements are added to obtain the heterodyne/dynamic characterization: a reference tunable laser source (1510-1575 nm), a 2x2 coupler, a 12 GHz photodetector and a fast scope (Tektronix, DP07000 100Gs/s). The TLS and SG-DBR laser outputs are combined at the 2x2 coupler; if their optical lasing frequency difference is less than the bandwidth of the photodetector (12 GHz), a beating signal is obtained, allowing the dynamic measurement of the lasing wavelength. Each current combination can be produced at a maximum speed of 10 μs per sample.

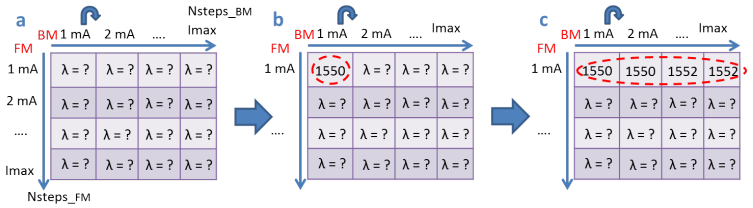

Figure 4. Raster current scanning. a) The tuning map starts as an empty matrix. b) The first FM,BM current combination is set and the lasing wavelength and SMSR are measured. c) The next column is measured until the matrix is filled.

2.3 Heterodyne measurement

The heterodyne/dynamic wavelength measurement is achieved by combining the TLS and SG-DBR laser in a 2x2 coupler. The TLS provides a constant reference wavelength value, while the SG-DBR laser is being dynamically tuned with a raster scanning pattern (Fig. 4). If at one moment in time it happens that the optical frequency ($f = c/\lambda$) difference between the TLS and the SG-DBR is within the bandwidth of the photodetector (12 GHz) an oscillating beating signal will be measured by the scope. With this beating signal, the automatic heterodyne method is able to provide time resolved optical spectrum analysis of fast laser wavelength switching where the wavelength range is determined by the TLS. The addition of a polarization controller is used to align the polarization of the TLS electric field with the SG-DBR field as two conditions must be met in order to obtain the beating signal: The spatial distributions must overlap and must not be orthogonal, while the polarization states must also not be orthogonal. The electronic signal is then recorded by a sampling oscilloscope.[32,33] The electric field of the wavelength switched laser is defined as an addition of N laser modes:

$$E_s = \sum_{n=1}^{N} a_s^n(t) e^{j2\pi \int_0^t \nu_s^n(\tau)d\tau + \phi_s^n} \tag{1}$$

where $\nu_s(t)$ is the time-dependent frequency, $a_s(t)$ the time dependent amplitude, and phase $\phi_s(t)$. The electric field of the TLS reference laser can be approximated by a single delta function at frequency ν_{lo}:

$$E_{lo} = a_{lo} e^{j2\pi\nu_{lo} + \phi_{lo}} \tag{2}$$

The electric field incident on the photodetector is $E = E_s + E_{lo}$ and its intensity is $I = EE^*$. Assuming the TLS and the frequency of one of the laser modes of the SG-DBR are within the bandwidth of the photodetector then the intensity of the beating signal is defined as:

$$I(t) = 2a_s(t)a_{lo}cos(\psi) + a_{lo}^2 + \sum_{n=1}^{N} a_s^n(t)^2 \tag{3}$$

where the beat signal phase, ψ, depends on the instantaneous frequency of the SG-DBR ($\nu_s(\tau)$) and is defined as:

$$\psi = 2\pi\Big(\int_0^t \nu_s(\tau)d\tau - \nu_{lo}t\Big) + \phi_s(t) - \phi_{lo} \tag{4}$$

The term $a_{lo}a_s(t)$ depends on the SG-DBR laser mode and determines the time varying envelope of the beat signal. In the setup of Fig. 3, the scope measures such an envelope from the photodetector while disregarding the phase of the beat signal. The bandwidth of the photodetector determines the allowable optical frequency differences that can be measured. The conversion from frequency to wavelength depends on the center wavelength according to:

$$\Delta\nu = \frac{c}{\lambda^2}\Delta\lambda \tag{5}$$

A beating signal can be measured according to the following experimental parameters: The DAQ is configured to have a sample rate of 100 kHz (sample/current combination produced every $t_{sample} = 10\mu s$), the total number of current combinations is given by $N_{stepsFM}{}^{*}N_{stepsBM}$ and the total matrix sweep time, $t_{sweep} = N_{stepsFM}{}^{*}N_{stepsBM} * t_{sample}$. For $N_{stepsFM} = N_{stepsBM} = 100$; $t_{sweep} = 100ms$. The beating signal is an oscillating signal whose frequency depends on the optical frequency difference of the signals as illustrated in Fig. 5a. Once a beating signal is obtained, its signal quality is measured by calculating its AC- Root Mean Square Voltage (AC-RMS), which can be directly obtained from the scope according to:

$$AC - RMS = \sqrt{\frac{\int_{start}^{end} (Waveform(t))^2 dt}{(End - Start) * SampleInterval}} \tag{6}$$

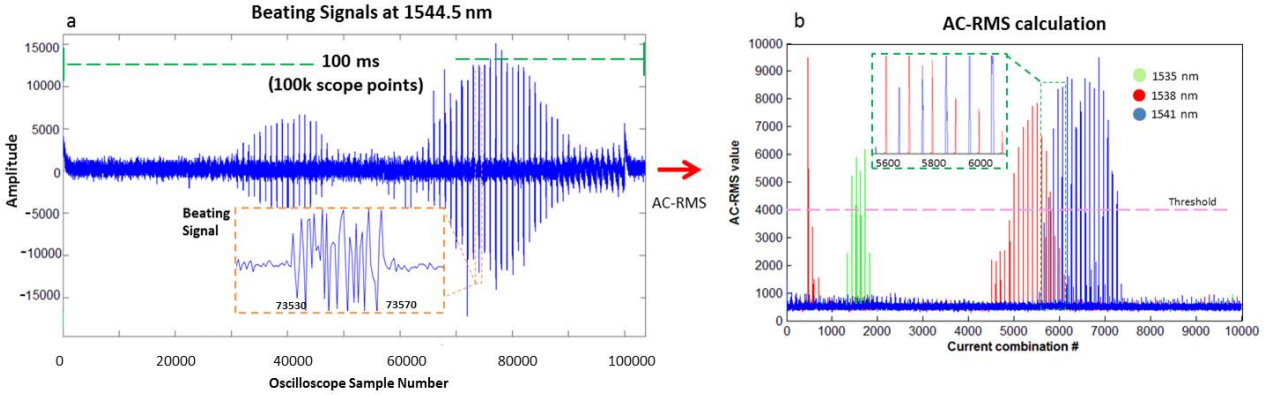

Figure 5. Beating signal AC-RMS. a) TLS set to lase at 1544.5 nm. Several beating signals are measured at the photodetector in an window of 100 ms and 100k sampling points. b) The AC-RMS is calculated for every 10 points of the scope for a total of 10000 current combinations (x-axis) in order to quantify the quality of the oscillating signal. Those that are above the reference threshold are remapped to a matrix.

In order to characterize the SG-DBR laser in its full tuning range, the TLS is tuned in steps of 0.1 nm, while the SG-DBR is being dynamically tuned. The AC-RMS per current combination is calculated for all reference wavelengths and then compared against a reference threshold level (Fig.5). If the AC-RMS value is above the threshold then the SG-DBR is lasing at an optical frequency difference of less than 12 GHz with respect to the TLS. All the current combinations that are above the threshold are then remapped to a matrix representing the pairs of current combinations as in Fig. 4 and are the combinations that make the SG-DBR laser lase at the reference wavelength. The following process is to select the adequate current combination per wavelength.

3. RESULTS

3.1 DC Results

DC characterization of the SG-DBR laser in terms of its lasing wavelength and SMSR was performed with the setup shown in Fig. 3. The wavelength tuning map (Fig.6a) relates the lasing wavelength as a function of both the BM and FM currents, for constant values of gain and phase. Three tuning sections can be identified: C1-3. Section C1 and C3 are limited in their tuning range and have very narrow tuning paths, hence they are discarded as it is not convenient to operate the laser in these sections. In contrast, C2 is the main tuning region which covers the whole tuning range and has a 'fanlike' shape where several wider tuning paths can be identified. With this pattern it is possible to find a tuning path with increasing wavelength in order to avoid being close to the borders of the neighboring paths and therefore reduce mode hopping. Such effect degrades the swept source lasing quality due to unexpected lasing wavelengths, hence this must be avoided. Notice, however, that for small current combinations the tuning paths are closer to each other, therefore increasing the probability of

mode hopping. This effect can be minimized by increasing the DAQ resolution and decreasing the electronic noise in the connections through electronic filtering and by placing the laser in a printed circuit board (PCB) where the impedance of each trace matches the electric impedance of each section of the laser. The SMSR Map (Fig.6b) shows that the laser had a remarkable single-mode operation (SMSR $>$ 30 dB) in region C2 as required for SS-OCT. With these maps, it was experimentally found that the laser had a useful tuning range of $\approx$ 60 nm (Fig.6c) at a center wavelength $\lambda_c = 1540$ nm and an average lasing power of 10 mW.

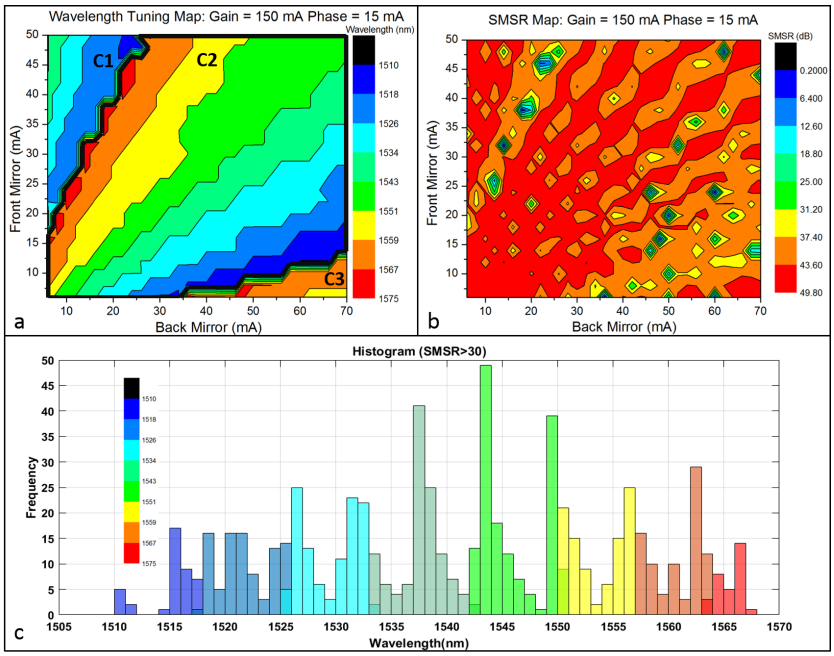

Figure 6. a) Wavelength Tuning Map with three tuning sections (C1-3). Tuning region C2 has clearly defined tuning paths. b) Side-mode supression ratio (SMSR) map. c) Wavelength histogram for values of SMSR>30. Laser configuration: Gain = 150 mA; Phase = 15 mA. FM: 6-50 mA (2 mA step); BM: 6-70 mA (2 mA step). OSA resolution: 0.1 nm

In order to study how the laser operates at different current combinations including the gain and phase, the SG-DBR laser was set to 27,000 different optical states using the same setup (Fig. 3). Each different optical state was obtained by combining the five input variables: BM (6-70, 2 mA step), FM (6-50, 2 mA step), phase (10-20, 2 mA step), gain (100-150 mA, 10 mA step) and SOA (100 mA). With this approach the data analysis is simplified as the system can be considered as a black box with five inputs and two outputs. Such results are shown in in Fig.7.

Fig.7a is a 3D surface plot that relates the wavelength as a function of the FM and BM currents. The same regions as well as the tuning paths are identified as in Fig. 6a. In order to cover each tuning path and obtain a linearly increasing wavelength, the BM current has to be increased significantly up to its maximum value compared to the FM current. Once the end of the tuning path has been reached both currents have to be changed abruptly (Fig.7b) Such condition can affect the performance of the laser by creating discontinuities in the output wavelength because the electronic transition can trigger several modes in between as the laser is fast enough to respond to fast current changes ($\approx$ 5 ns). After having an abrupt current change the laser needs time to stabilize and therefore a crucial design parameter is to have electronics that are fast enough to transition from a high to a low value of current with the least possible noise and current spikes. The quality of the optical signal can preserved by using the SOA as an optical shutter so that the light is absorbed in such section during the transition. Fig. 7c,d show three wavelength and SMSR tuning maps of region C2 at three different phase levels. Wavelength fine tuning is achieved by stepping the phase current at small intervals ($<$ 1 mA).

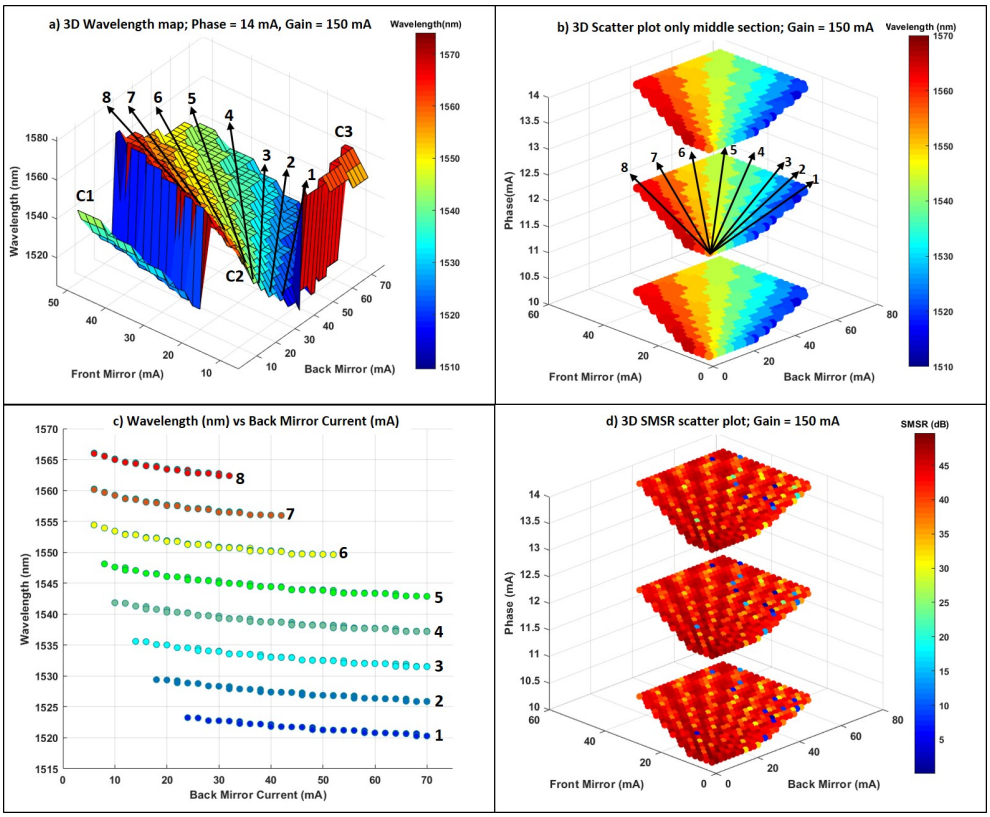

Figure 7. a) 3D wavelength surface plot. Phase = 14 mA; Gain = 150 mA b) 3D scatter plot at three phase levels (10-14, 2 mA step) with only C2 middle tuning region. Eight main tuning paths can be identified. c) Wavelength in nm as a function of BM current. Eight tuning paths are also identified. d) 3D SMSR scatter plot at three phase levels (10-14, 2 mA step).

3.2 AC results

DC characterization provided a complete understanding of how the laser behaves as a function of the input currents. However, SS-OCT requires swept sources to be swept in orders of 100-200 kHz, hence AC dynamic characterization is required in order to know how stable is the instantaneous lasing wavelength, how repetitive are the wavelength sweeps and what current combinations are necessary to tune to laser in a linearly increasing way. AC characterization of the SG-DBR laser in terms of its lasing wavelength was performed with the setup shown in Fig. 3. The results are shown in Fig.8 and Fig.9.

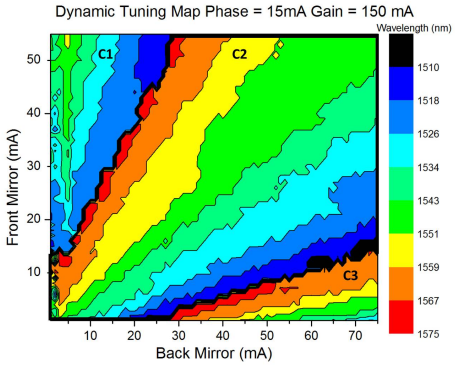

Figure 8. Dynamic Tuning Map measured at 100 kHz (10 μs per current combination)

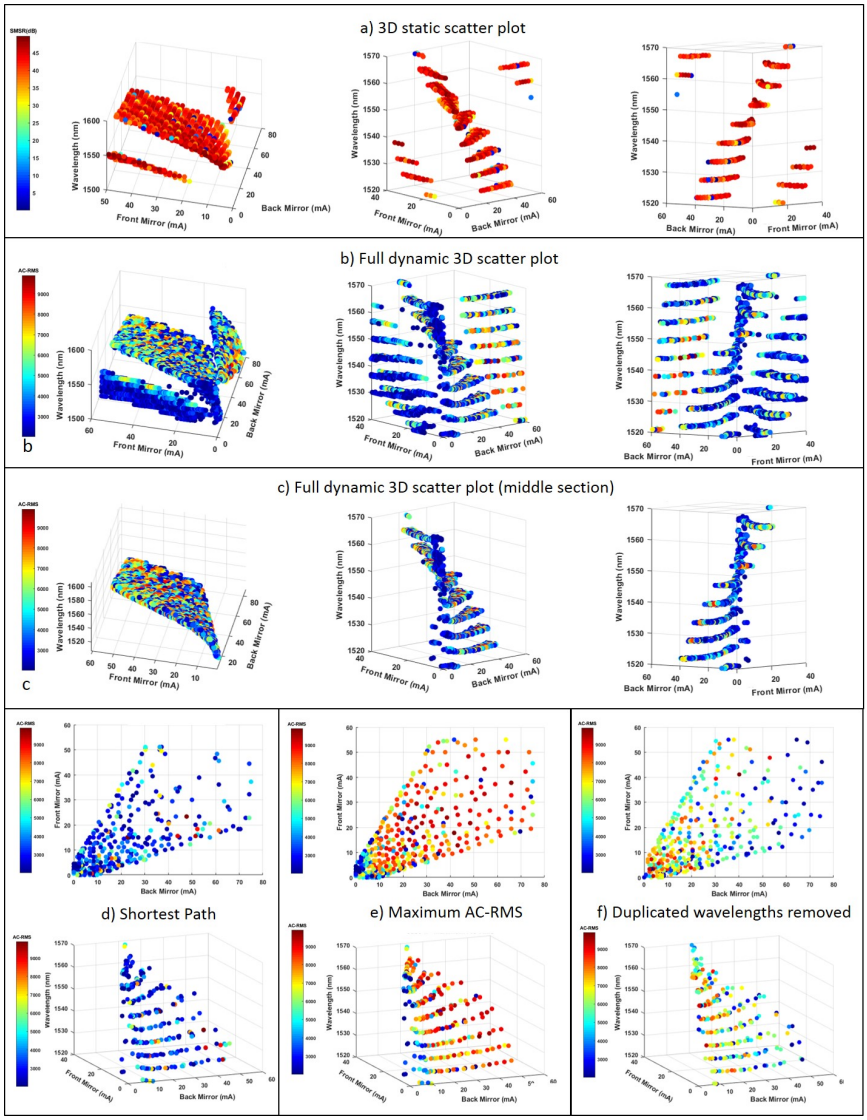

Figure 9. AC characterization at 100 kHz (10 μs per current combination) a)3D static scatter plot b)Full dynamic 3D scatter plot with three tuning regions (7000 tuning points) c)Tuning points only from the middle region (3428 tuning points) d)Shortest Path (379 points) e)Maximum AC-RMS (379 points) f)Duplicated wavelengths removed (379 points)

Fig.8 is a dynamic tuning map measured at 100 kHz (10 μs per current combination). Notice that its behavior is similar to its DC version (Fig.6) as three tuning regions are identified, where the central region (C2) contains several tuning paths in linearly increasing wavelength. Despite their similarity, the AC characterization is completely necessary as it was experimentally observed that the laser has a hysteretic behavior, meaning that in order to reproduce the same tuning map it is required to follow the same tuning conditions in terms of sweeping speed, current steps, maximum currents and temperature. When such conditions were not fully met, different dynamic tuning maps were obtained.

Using the AC-RMS as a reference value to quantify the beating signal quality allowed determination of the lasing wavelength per current combination (Fig.5), such results are shown in Fig.9b-f. Instead of having a tuning map, a 3D scatter plot represents the wavelength as a function of the front and back mirror currents, where the color code is the calculated AC-RMS (red represents a better quality signal). These plots are very relevant as they present many similarities with the previously obtained DC maps (Fig.7, Fig.9a) Fig.9b presents three main tuning regions, as previously found. Each tuning path can also be identified, notice however this tuning path has

a higher density of points to be chosen from, hence a computer program was written to select only one current combination per wavelength according to the following criteria:

1. Avoid abrupt current changes of bias current.
2. Choose points that are as close as possible to the center of the tuning paths and not at the edges in order to avoid mode hopping.
3. Choose a path with linearly increasing wavelength, e.g., with the same wavelength step.

In order to meet the 1^{st} criteria only the points of the central region are kept (Fig.9c, 3428 tuning points). With this point filtering, the only abrupt current changes that will happen is when going from the end of a tuning path, to the beginning of the next one. The following step is to choose only one current combination per wavelength, for this reason three solutions were proposed: Chose the points with the shortest path, maximum AC-RMS and remove the duplicate wavelengths (Fig.9d-f, 379 tuning points). The 1^{st} solution reduces abrupt current changes, however it was observed that the lowest AC-RMS quality points are chosen (blue points), not only that but there is a high density of current combinations for low currents which will cause mode-hopping. The 2^{nd} solution automatically chooses the highest quality AC-RMS between a group of points, there is also a high density of points for low values of current. The 3^{rd} solution removes all current combination duplicates and keeps only one. Most of the chosen points are neither the highest quality nor lowest quality point but an intermediate value. What can be observed from the three cases is that most of the dynamic tuning for this SG-DBR laser happens in a window of 20 mA for both FM and BM, hence the relevance of being able to produce current values as close as possible to the desired values and decreasing the electronic noise as much as possible. A 'tuning dictionary' is obtained with the chosen points. Such points are put into a list and the laser is swept with the chosen current combinations (379 tuning points).

4. DISCUSSION

DC characterization provided a broad understanding of the behavior of the SG-DBR laser allowing identification of the central tuning region as well as its tuning paths. It is also possible to determine the tuning range, central wavelength, SMSR, average lasing power and the lower and upper limits for the mirror tuning currents. An advantage of the proposed setup is that different tunable laser architectures can be characterized as the whole characterization process has been automated, therefore the setup is not limited only to SG-DBR architectures. Despite the broad picture given by the DC characterization it is absolutely necessary to perform the heterodyne/AC measurement of the laser.

The final outcome of the heterodyne/AC characterization were the tuning dictionaries which were then tested and the following behavior observed. Invalid points in the sweep and large stitching noise were two important limitations that need to be compensated in order to use the SG-DBR laser as a swept source. Invalid points in the sweep were observed when the instantaneous lasing wavelength drifted from the expected value. E.g, the instantaneous lasing wavelength for the shortest path and maximum AC-RMS deviated from the expected value for certain current combinations. A solution to replace the invalid points is to use this point as a 1^{st} reference, replace it with a neighboring value, reproduce the sweep and observe the wavelength stability. This process shall be repeated until a stable point is found. Large stitching noise and large amounts of optical noise was associated with abrupt changes in injection currents, especially when going from the end of one tuning path to the start of the following one, hence reducing the quality of the linear sweep since undesired wavelengths affect the quality of an OCT image. Such behavior is due to the mode-hopping of the laser as the injection currents abruptly change from one set to a completely different one. A solution to limit the stitching noise is to add a feedback loop to know the instantaneous lasing wavelength. When mode-hopping is detected in the laser, the feedback loop shall compensate it by dynamically changing the input currents of the laser in order to stabilize the lasing wavelength. When implementing this solution, one has to be careful of properly designing the control system, otherwise the system can become unstable. Other adverse effects are due to the high density of points in the lower left window of the tuning paths (thus being sensitive to electronic noise) and when one current combination is too close to

the border of a tuning path. This effect was observed in real time at the scope; several wavelength 'flashes' were observed, therefore the instantaneous wavelength was not entirely stable.

A relevant observation during the dynamic tuning of the laser was that the quality and stability of the instantaneous wavelength was highly dependent on the previous optical state, hence when the same path was reproduced the signal quality was improved compared to choosing the same current combination but having different previous optical states. Such behavior is due to the hysteresis of the laser. A solution to this problem is to use the tuning dictionary as a reference/starting point and then fine tune the values of the currents in order to find a path with better optical performance; such a process is then repeated until a stable configuration is obtained. This process was tested with the tuning dictionary by selecting alternatives from the duplicate wavelengths. This improved performance but the lasing wavelength was still unstable when changing from one tuning path to another.

In order for the SG-DBR laser to become the swept source for a SS-OCT several considerations have to be taken into account: The laser sections are sensitive enough to detect electric noise coming from the control electronics, therefore when the laser is operating near the border of two tuning regions unstable mode-hopping is present. This behavior can be compensated by choosing points closer to the center of the tuning paths and can be practically accomplished by adding a feedback loop of the wavelength in order to fine tune the phase section to obtain the desired wavelength. This concept can also be applied during the transition of abrupt current changes and control of the current in the SOA so that instead of letting the laser light being transmitted it is absorbed. Another relevant parameter to have a stable linear sweep is the temperature of the device. Different current densities being injected to the semiconductor structures at high speed rates produces different local temperatures per section, the section with the highest temperature will change the temperature of the adjacent section, hence when reproducing a tuning dictionary the temperature has to be the same as when it was firstly measured, otherwise the lasing wavelength will not be as expected. In this setup, the temperature of the SG-DBR laser was only controlled with the TEC.

5. CONCLUSION

An automated heterodyne method has been proposed as a tool to characterize all-semiconductor akinetic SG-DBR lasers in DC and AC performance. With this method, swept sources researchers will be able to know the useful tuning range, central wavelength, SMSR and average lasing power for DC operation. Also, it will be possible to create specific tuning dictionaries for different laser architectures in order to obtain linear sweeps as required by SS-OCT. The invalid points and stitching noise can be measured and then compensated by repeating the whole measurement process. Each laser has a unique behavior, therefore having a technique to automatically characterize them will be essential for swept source developers as they will be able to discriminate which lasers have the potential to be the core of a swept source OCT system.

ACKNOWLEDGMENTS

Funding was from the European Union H2020 PICCOLO Project - Multimodal highly-sensitive photonics endoscope for improved in-vivo colon cancer diagnosis and clinical decision support (https://www.piccolo-project.eu/). The authors also acknowledge Liam Barry from Dublin City University (DCU) for providing the JDSU Agile laser.

REFERENCES

[1] Drexler, W. and Fujimoto, J., [*Optical Coherence Tomography: Technology and Applications*], Springer Publishing, Berlin, Heidelberg (2008 (2nd edition)).

[2] Huang, D., Swanson, E., Lin, C., Schuman, J., Stinson, W., Chang, W., Hee, M., Flotte, T., Gregory, K., Puliafito, C., and Fujimoto, J., "Optical coherence tomography," *Science* **254**, 1178–1181 (Nov 1991).

[3] Fercher, A., Hitzenberger, C., Kamp, G., and El-Zaiat, S., "Measurement of intraocular distances by backscattering spectral interferometry," *Optics communications* **117**, 43–48 (May 1995).

[4] Wojtkowski, M., Leitgeb, R., Kowalczyk, A., Bajraszewski, T., and Fercher, A., "In vivo human retinal imaging by fourier domain optical coherence tomography," *Journal of Biomedical Optics* **7(3)**, 457–463 (July 2002).

[5] Leitgeb, R., Hitzenberger, C., and Fercher, A., "Performance of fourier domain vs time domain optical coherence tomography," *Optics Express* **11(8)**, 889–894 (March 2003).

[6] Chinn, S. and E. Swanson, J. F., "Optical coherence tomography using a frequency-tunable optical source," *Optics Letters* **22**, 340–342 (March 1997).

[7] Golubovic, B., Bouma, B., Tearney, G., and Fujimoto, J., "Optical frequency-domain reflectometry using rapid wavelength tuning of a cr4+:forsterite laser," *Optics Letters* **22**, 1704–1706 (November 1997).

[8] Lexer, F., Hitzenberger, C., Fercher, A., and Kulhavy, M., "Wavelength-tuning interferometry of intraocular distances," *Applied Optics* **36, No. 25**, 6548–6553 (September 1997).

[9] Hiratsuka, H., Kido, E., and Yoshimura, T., "Simultaneous measurements of three-dimensional reflectivity distributions in scattering media based on optical frequency-domain reflectivity," *Optics Letters* **23, No. 18**, 1420–1422 (September 1998).

[10] DeBoer, J., Leitgeb, R., and Wojtkowski, M., "Twenty-five years of optical coherence tomography: the paradigm shift in sensitivity and speed provided by fourier domain oct," *Biomedical Optics Express* **Vol. 8, No. 7**, 3248–3280 (July 2017).

[11] Drexler, W., Liu, M., Kumar, A., Kamali, T., Unterhuber, A., and Leitgeb, R., "Optical coherence tomography today: speed, contrast, and multimodality," *Biomedical Optics* **19, No. 7**, 071412:1–34 (2014).

[12] Klein, T. and Huber, R., "High-speed oct light sources and systems," *Biomedical Optics Express* **8, No. 2**, 828–859 (Feb. 2017).

[13] Derickson, D., Bernacil, M., DeKelaita, A., Maher, B., O'Connor, S., Sysak, M., and Johanssen, L., "Sgdbr single-chip wavelength tunable laser for swept source oct," *Proc. SPIE* **6847** (Feb 2008).

[14] Minneman, M., Ensher, J., Crawford, M., and Derickson, D., "All-semiconductor high-speed akinetic swept-source for oct," *Optical Sensors and Biophotonics* **Vol. 8311** (2011).

[15] Ensher, J., Boschert, P., Featherston, K., Huber, J., Crawford, M., Minneman, M., Chiccone, C., and Derrickson, D., "Long coherence length and linear sweep without an external optical k-clock in a monolithic semiconductor laser for inexpensive optical coherence tomography," *Proc. SPIE* **8213** (2012).

[16] Coldren, L., "Monolithic tunable diode lasers," *J. Sel. Top. Quantum Electronics* **6**, 988–999 (Nov 2000).

[17] Choi, D., Yoshimura, R., and Ohbayashi, K., "Tuning of successively scanned two monolithic vernier-tuned lasers and selective data sampling in optical comb swept source optical coherence tomography," *Biomedical Optics Express* **Vol. 4, No. 12**, 2962–2987 (December 2013).

[18] AxsunTechnologies, "OCT Swept Laser Engines." Available at http://www.axsun.com/oct-swept-lasers. (Accessed: 04 December 2018).

[19] EXALOS, "Swept Sources." Available at http://www.exalos.com/swept-sources/. (Accessed: 04 December 2018).

[20] NTT, "200-KHz Swept Light Source for OCT Imaging." Available at http://www.ntt-at.com/product/ktn_oct/. (Accessed: 04 December 2018).

[21] Santec, "Laser for Swept Source OCT." Available at http://www.santec.com/en/products/oct/lasers-for-swept-source-oct. (Accessed: 04 December 2018).

[22] Thorlabs, "1300 nm MEMS-VCSEL Swept Source OCT Imaging System, 100 KHz." Available at https://www.thorlabs.com/thorproduct.cfm?partnumber=OCS1310V1. (Accessed: 04 December 2018).

[23] Superlum, "Swept Wavelength Tunable Semiconductor Lasers, Broadsweepers." Available at https://www.superlumdiodes.com/broadsweepers.htm. (Accessed: 04 December 2018).

[24] Optores, "Next generation FDML Laser." Available at https://optores.com/index.php/products/31-next-generation-fdml-laser. (Accessed: 04 December 2018).

[25] InsightPhotonics, "Insight Akinetic Swept Lasers Enabling OCT and SS-OCT Angiography." Available at http://www.sweptlaser.com/content/insight-akinetic-swept-lasers-enabling-oct-and-ss-oct-angiography. (Accessed: 04 December 2018).

[26] Bonesi, M., Minneman, M. P., Ensher, J., Zabihian, B., Sattmann, H., Boschert, P., Hoover, E., Leitgeb, R. A., Crawford, M., and Drexler, W., "Akinetic all-semiconductor programmable swept-source at 1550 nm and 1310 nm with centimeters coherence length," *Opt. Express* **22**, 2632–2655 (Feb 2014).

[27] Chen, Z., Liu, M., Minneman, M., Ginner, L., Hoover, E., Sattmann, H., Bonesi, M., Drexler, W., and Leitgeb, R., "Phase-stable swept source oct angiography in human skin using an akinetic source," *Biomedical Opt. Express* **7, No. 8**, 3032–3048 (Aug 2016).

[28] Salas, M., Augustin, M., Felberer, F., Wartak, A., Laslandes, M., Ginner, L., Niederleithner, M., Ensher, J., Minneman, M., Leitgeb, R., Drexler, W., Levecq, X., Schmidt-Erfurth, U., and Pircher, M., "Phase-stable swept source oct angiography in human skin using an akinetic source," *Biomedical Opt. Express* **7, No. 8**, 3032–3048 (Aug 2016).

[29] Buus, J., Amann, M., and Blumenthal, D., "Widely tunable monolithic laser diodes in tunable laser diodes and related optical sources," *IEEE* , 169–219 (2005).

[30] Sarlet, G., Morthier, G., and Baets, R., "Control of widely tunable ssg-dbr lasers for dense wavelength division multiplexing," *Lightwave Technology* **18, No. 8**, 3032–3048 (Aug 2000).

[31] James, B., *High Speed Wavelength Tuning of SGDBR Lasers for Optical Coherence Tomography Applications*, master's thesis, Electrical Engineering Department Faculty of California Polytechnic State University, San Luis Obispo.

[32] Engelstaedter, J., Roycroft, B., Peters, F., and Corbett, B., "Heterodyne method for time resolved spectral analysis of fast laser wavelength switching," *IEEE Photonics Technology Letters* **21, No. 20**, 1517–1519 (Oct 2009).

[33] Baney, D., Szafraniec, B., and Motamedi, A., "Coherent optical spectrum analyzer," *IEEE Photonics Technology Letters* **14, No. 3**, 355–357 (March 2002).